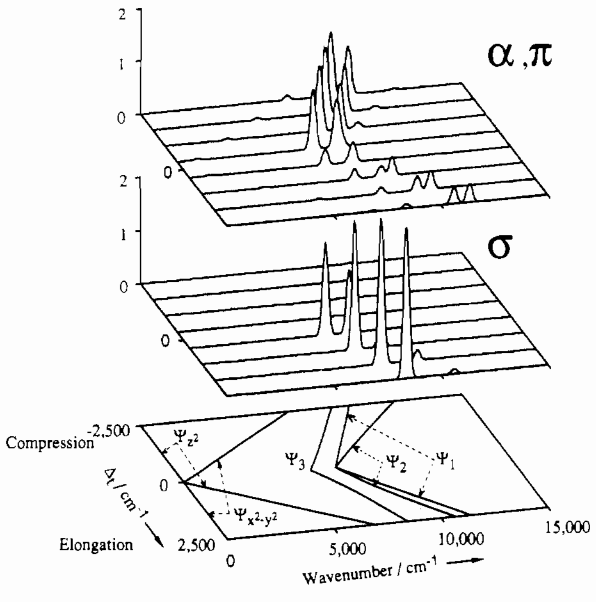

Figure 3. Calculated magnetic dipole strengths as a function of Δ_t for α, $\pi(H\|xy)$, and σ $(H\|z)$ polarizations. The "cubic" field is held fixed at $\Delta = 6500$ cm^{-1} and $k = 0.86$. The intensity is given in units of $\mu_B{}^2$.

methods previously given,[9] with the "cubic" part of the ligand field held constant at $\Delta = 2\sigma_\perp + \sigma_\| + {}^4/_3(2\pi_\perp + \pi_\|)$ and the effect of the tetragonal field on the e_g orbitals given by $\Delta_e = 2(\sigma_\perp - \sigma_\|) \approx 3\Delta_t$. An orbital reduction factor of $k = 0.86$ was used with the reduced spin-orbit coupling constant of $\lambda = 714$ cm^{-1}.

The most striking features of Figure 3 are that there is only a *single* strong origin for elongated octahedra, while there are *two* origins of comparable intensity for compressed octahedra. Again, this is strong evidence that the spectra of Figure 1 are due to tetragonally compressed $CuF_6{}^{4-}$ complexes. However, it must be emphasized that Figure 3 implies "vertical" electronic transitions. The observed intensity also depends on the overlap of the ground- and excited-state zero-point vibrational functions. This overlap is very sensitive to the relative displacement of the minima. The vibrational functions should be approximately localized about the minima of their respective potentials, and small relative displacements of these minima should greatly affect the relative vibronic reduction factors. It remains to show that these reduction factors strengthen the intensity argument.

For the elongated case, the equilibrium geometry of the ground state should correspond to an elongation greater than that of any of the $^2T_{2g}$ excited states. This follows from the greater effect a tetragonal distortion has on the e_g compared to the t_{2g} orbitals, or more simply $e_\sigma > e_\pi$. The slopes of the energy levels in Figure 2 require that the minima of the states Ψ_3, Ψ_2, and Ψ_1 be increasingly displaced with respect to the ground state. Therefore, relative to the strong origin of Ψ_3, the origins of the Ψ_2 and Ψ_1 states should be even weaker than actually shown in Figure 3. This is exactly what was observed for K_2CuF_4, where the Ψ_2 origin was found to have only $\sim{}^1/_{60}$th of the intensity of the Ψ_3 origin, while the Ψ_1 origin was not even observed.

Similarly, the ground state in the compressed case is expected to have a more compressed geometry than any of the excited states. The energy levels of the two lowest excited states, Ψ_3 and Ψ_1, have a similar slope and therefore have *similar* displacements.

Therefore, for an elongated octahedron, only *one* main origin would be expected when the magnetic vector of the incident light is parallel to the tetragonal axis $(H\|z)$ and no origins would be expected for $H \perp z$. Conversely, for a compressed octahedron, no origin would be expected for $H\|z$, while *two* origins of comparable intensity would be expected for $H \perp z$. The mere fact that two electronic origins were observed in the low-temperature absorption spectrum of $KCuAlF_6$ shows that the copper center is in a compressed geometry. The energy separation of these origins gives an estimate of the size of the distortion.

The data in Table I suggest that the $CuF_6{}^{4-}$ center in $KCuAlF_6$ should have a geometry similar to that found in the doped $Ba_2Zn(Cu)F_6$ system. The Ba_2ZnF_6 compound has the bond lengths[11] 196 (×2) and 205 pm (×4), whereas for $KCuAlF_6$ the reported[5] bond lengths are 187, 188, and 212 pm (×4). This implies that the six-coordinate Cu(II) complexes do not necessarily adopt the exact geometry of the host lattice. Rather, the magnitude of the tetragonal distortion is intrinsic to the Cu(II) ion from the $E \otimes \epsilon$ Jahn-Teller effect, while the role of the crystal lattice is to determine the sign of the distortion. The structure of the analogous $KZnAlF_6$ compound is also compressed[12] with the bond lengths 194, 196, 206 (×2), and 211 pm (×4), and so it appears that the sign of the tetragonal distortion is also determined by lattice forces in undiluted copper(II) compounds.

The size of the Jahn-Teller distortion in the ground state, given by[1] ρ_0 $[=(\sum_i(r_i - \bar{r})^2)^{1/2}] = 28$ pm, is smaller than that found for K_2CuF_4, $\rho_0 = 33$ pm, which is consistent with simple $E \otimes \epsilon$ Jahn-Teller models where the warping of the "Mexican hat" potential causes ρ_0 to be larger for an elongated compared to a compressed geometry.[13]

Conclusions

The $CuF_6{}^{4-}$ centers in $KCuAlF_6$ have been shown unambiguously to be compressed octahedra by low-temperature absorption measurements. This is in agreement with the published crystal structure[5] and represents one of the few pure compounds known in which copper(II) adopts a compressed geometry.[5,14] Criteria for spectroscopically distinguishing between compressed and elongated octahedra have been given. Such spectrostructural relationships can be useful in cases where the crystal structure determination may be complicated by twinning or antiferrodistortive ordering.

Acknowledgment. We thank Dr. M. A. Hitchman for helpful discussions and Prof. R. Hoppe for providing the single crystals.

---

(9) Riley, M. J.; Dubicki, L.; Moran, G.; Krausz, E. R.; Yamada, I. *Inorg. Chem.* **1990**, *29*, 1614.

(10) Reinen, D.; Steffen, G.; Riley, M. J.; Hitchman, M. A.; Stratemeier, H. To be submitted for publication.

(11) von Schnering, H. G. *Z. Anorg. Allg. Chem.* **1967**, *353*, 14.

(12) Wingefeld, G. Ph.D. Thesis, Institute for Inorganic and Analytical Chemistry, Giessen, West Germany, 1984.

(13) Deeth, R. J.; Hitchman, M. A. *Inorg. Chem.* **1986**, *25*, 1225.

(14) Effenberger, H. *Z. Kristallogr.* **1989**, *188*, 43. Basso, R.; Palenzona, A.; Zefiro, L. *Neues Jahrb. Mineral., Monatsh.* **1988**, 385.

Contribution from the Laboratoire de Chimie Théorique,
Université de Paris-Sud, 91405 Orsay, France

Conformation of H_2 on Dinuclear Complexes: Attractive Effect of a Cis Hydride

Sarah A. Jackson and Odile Eisenstein*

Received January 31, 1990

The nonclassical coordination of H_2 to mononuclear transition-metal complexes has been established for a number of different metal centers and studied via a variety of experimental and theoretical techniques.[1] However, examples of dinuclear transition-metal complexes involving this novel ligand are relatively rare.[2,3] The aim of this work is to show that the nature of the

---

(1) See for example: (a) Kubas, G. J. *Acc. Chem. Res.* **1988**, *21*, 120. (b) Crabtree, R. H.; Hamilton, D. G. *Adv. Organomet. Chem.* **1988**, *28*, 299.

(2) (a) Arliguie, T.; Chaudret, B.; Morris, R. H.; Sella, A. *Inorg. Chem.* **1988**, *27*, 599. (b) Hampton, C.; Dekleva, T. W.; James, B. R.; Cullen, W. R. *Inorg. Chim. Acta* **1988**, *145*, 165. (c) Joshi, A. M.; James, B. R. *J. Chem. Soc., Chem. Commun.* **1989**, 1785.

(3) Hampton, C.; Cullen, W. R.; James, B. R.; Charland, J. *J. Am. Chem. Soc.* **1988**, *110*, 6918.

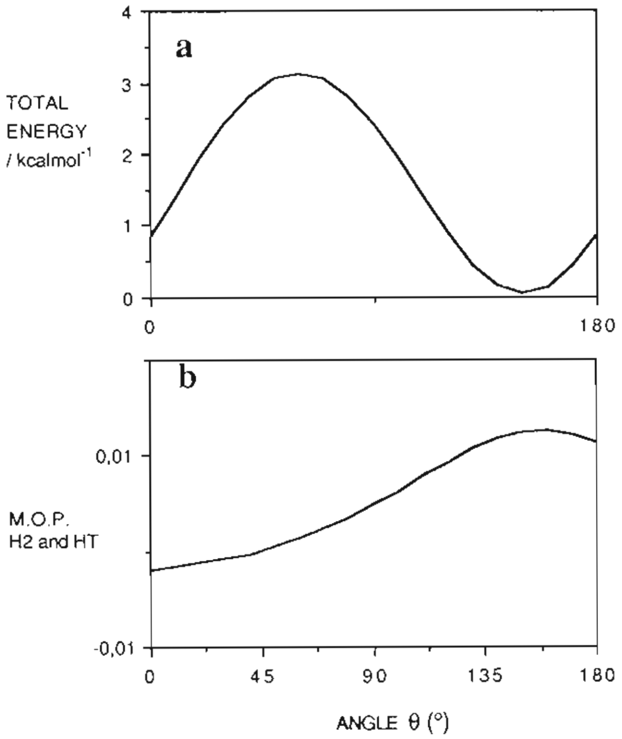

Figure 1. Variation in (a) the total energy and (b) the MOP between H2 and HT as dihydrogen is rotated on **2**. Angle θ is the angle between the H–H and Ru1⋯Ru2 directions.

bonding between H_2 and a dinuclear moiety is governed by processes similar to those of a mononuclear complex.

H_2 Coordination on $(P\text{-}N)(\eta^2\text{-}H_2)Ru(\mu\text{-}Cl)_2(\mu\text{-}H)Ru(PR_3)_2(H)$

The first X-ray crystal structure confirming the presence of nonclassically coordinated H_2 in a dinuclear complex was recently reported for the complex $(P\text{-}N)(\eta^2\text{-}H_2)Ru(\mu\text{-}Cl)_2(\mu\text{-}H)Ru(PR_3)_2(H)$ (**1**) (P-N = $Fe(\eta^5\text{-}C_5H_3(CHMeNMe_2)P(i\text{-}Pr)_2\text{-}1,2)(\eta^5\text{-}C_5H_5)$; R = Ph).[3] The structure of **1** is derived from a pair of edge-sharing distorted octahedra. The bridging hydride (HB) is located on the same side of the complex as both the terminal hydride (HT) and H_2. Molecular H_2 is found to orient itself on the metal center in a direction roughly equivalent with the Ru1–HB direction. A fast exchange process is observed on the NMR time scale at ambient temperatures between H_2 and HB, and a slower exchange between HB and HT. We were especially interested in **1**, since we felt that these exchange processes could be facilitated by so-called cis interactions similar to those that we have proposed in mononuclear olefin and H_2 complexes.[4] Our studies have shown that the presence of a hydride cis to such ligands may influence their conformation. This effect is caused by a high-lying orbital, representative of a metal hydride orbital, interacting with an empty molecular orbital of the cis ligand. A related effect has been found in polyhydrides.[5]

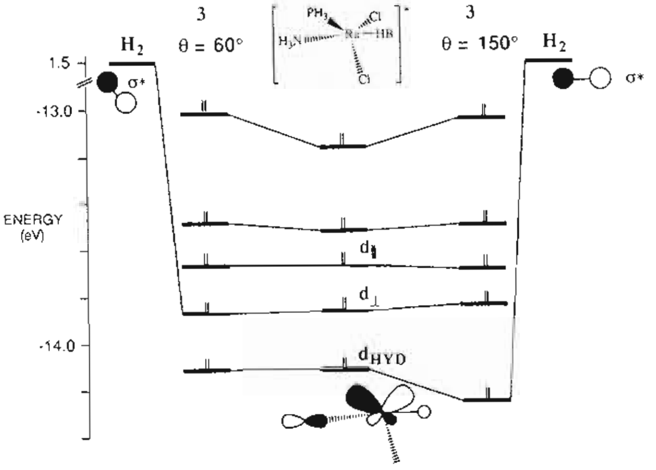

Figure 2. Interaction diagram for H_2 and $(Ru(PH_3)(NH_3)(Cl)_2H)^-$ at $\theta = 60°$ (total energy maximum) and $\theta = 150°$ (total energy minimum). The unlabeled orbitals are mainly chlorine lone pairs, which interact in a destabilizing manner with σ_{HH}. For clarity, the weak interaction between $d_{\parallel}$ and σ^* at $\theta = 150°$ is not indicated by a line.

Table 1. Overlaps and MOPs between Fragment Molecular Orbitals of $[(PH_3)(NH_3)Ru(Cl)_2(H)]^-$ and H_2 in 3 at $\theta = 150°$ (Total Energy Maximum) and at $\theta = 60°$ (Total Energy Minimum)

	$\theta = 150°$	$\theta = 60°$
	Overlap	
$\langle\sigma_{HH}\vert LUMO\rangle$	0.433	0.431
$\langle\sigma^*_{HH}\vert d_{\parallel}\rangle$	0.085	0.010
$\langle\sigma^*_{HH}\vert d_{\perp}\rangle$	0.013	0.067
$\langle\sigma^*_{HH}\vert d_{HYD}\rangle$	0.185	0.041
	MOP	
$\langle\sigma^*_{HH}\vert d_{\parallel}\rangle$	0.016	0.000
$\langle\sigma^*_{HH}\vert d_{\perp}\rangle$	0.000	0.013
$\langle\sigma^*_{HH}\vert d_{HYD}\rangle$	0.066	0.003

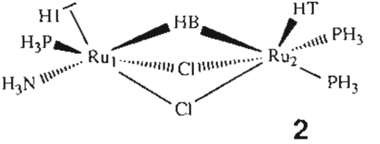

2

We have carried out extended Hückel molecular orbital calculations (EHMO)[6] adapting the X-ray crystal structure of **1** to the model complex $(PH_3)(NH_3)(\eta^2\text{-}H_2)Ru(\mu\text{-}Cl)_2(\mu\text{-}H)Ru(PH_3)_2(H)$ (**2**), using basis set parameters for HT that are a better representation of a hydride[7] and normal hydrogen parameters for all other H atoms present. We have examined the rotation of H_2 about an axis through the Ru1–H_2 bond vector. The variation of the total energy with the angle between the H–H direction and the Ru1⋯Ru2 direction (θ) is presented in Figure 1a. No relaxation of the geometry of the dinuclear fragment was permitted during the rotation of H_2, which introduces no unusually short H_2–ligand nonbonding contacts. An energy minimum is obtained at $\theta = 150°$, which is in good agreement with the experimental θ value (175°). The barrier to rotation of H_2 is calculated to be 3.1 kcal mol^{-1}, which has the same order of magnitude as rotational barriers in mononuclear H_2 complexes.[4b,8] The energy minimum in **2** coincides with a maximum in Mulliken overlap population (hereafter MOP) between the closest H center of H_2 and HB (0.013) (Figure 1b) and also a minimum in distance between these

---

(4) (a) Johnson, T. J.; Huffman, J. C.; Caulton, K. G.; Jackson, S. A.; Eisenstein, O. *Organometallics* **1989**, *8*, 2073. (b) Van Der Sluys, L. S.; Eckert, J.; Eisenstein, O.; Hall, J. H.; Huffman, J. C.; Jackson, S. A.; Koetzle, T. F.; Kubas, G. J.; Vergamini, P. J.; Caulton, K. G. *J. Am. Chem. Soc.* **1990**, *112*, 4831.

(5) Jackson, S. A.; Eisenstein, O. *J. Am. Chem. Soc.*, in press.

(6) EHMO calculations were carried out by using the weighted H_{ij} formulation; Ammeter, J. H.; Bürgi, H.-B.; Thibeault, J. C.; Hoffmann, R. *J. Am. Chem. Soc.* **1978**, *100*, 3686. The parameters for Ru were taken from: Thorn, D. L.; Hoffmann, R. *Inorg. Chem.* **1976**, *17*, 126. The geometries of **2** and **3** were adapted from the structure in ref 3 by replacement of P-N with separate PH_3 and NH_3 groups and PR_3 by PH_3. Calculations using regular octahedral structures of **1** as starting points were carried out but were found to be inconclusive, since the conformation of H_2 is highly sensitive to distortions around the metal center;[4b] these results are not discussed here. A regular octahedral structure was used for **5**, except for the hydride bridges (see text), and the distances used were Ru–P = 2.24, P–H = 1.40, Ru–HB = 1.64, Ru–H_2 = 1.44, and H–H = 0.84 Å.

(7) We have previously proposed the use of hydride parameters in the basis set of EHMO calculations on transition-metal terminal hydrides[4] different from those used for normal hydrogens. The parameters used for terminal H in this work are $H_{ii} = -11.6$ eV and $\zeta = 1.0$, compared to normal H parameters that are $H_{ii} = -13.6$ eV and $\zeta = 1.3$, which have been used for all other H atoms in the complex (including molecular H_2 and bridging hydrides). The "hydridic" parameters provide a more diffuse H 1s orbital, lying at higher energy.

(8) (a) Eckert, J.; Kubas, G. J.; Dianoux, A. J. *J. Chem. Phys.* **1988**, *88*, 466. (b) Jean, Y.; Eisenstein, O.; Volatron, F.; Maouche, B.; Sefta, F. *J. Am. Chem. Soc.* **1986**, *108*, 6587. (c) Hay, P. J. *Ibid.* **1987**, *109*, 705.

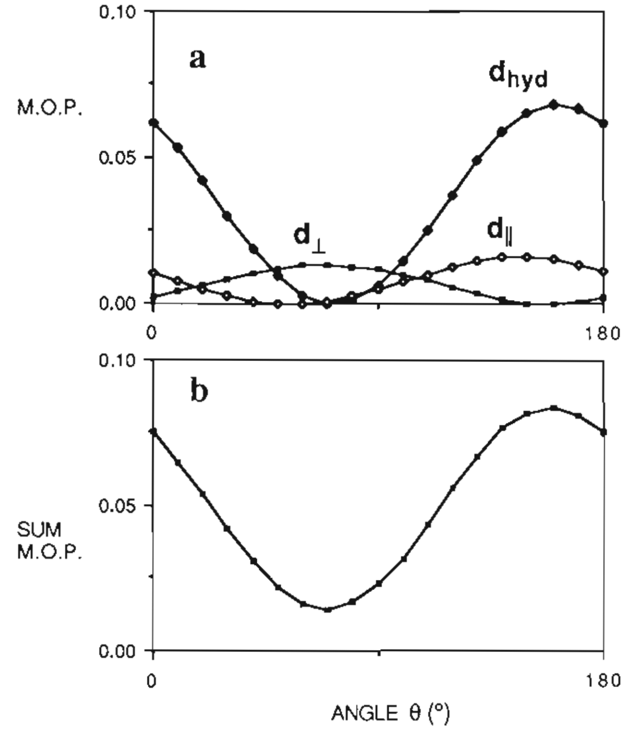

Figure 3. Variation in MOP of the d orbitals with σ^*_{HH}, (a) separately and (b) summed, of $(Ru(PH_3)(NH_3)(Cl)_2H)^-$ with changing θ.

two atoms (2.00 Å). The MOP between HB and HT is 0.014 (HB···HT distance = 2.09 Å).[9] These MOP values are typical of those we have found between H centers in other cis-hydride-/nonclassical H_2[4] and cis-dihydride[5] complexes.

This evidence does indeed point toward a bonding description involving a *cis* interaction. However, the large number of atoms in **1**, combined with the large extent of the distortion from the octahedral environments of the two metal centers, leads to a complicated molecular orbital analysis. The analysis can be simplified considerably if the complex is modeled on a mononuclear complex.

The model mononuclear complex $[(PH_3)(NH_3)(\eta^2\text{-}H_2)Ru(Cl)_2(H)]^-$ (**3**) has bond lengths and angles analogous to those of the equivalent atoms in **2**. Normal hydrogen parameters have

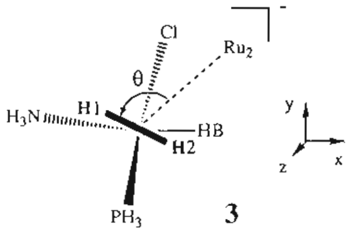

3

been used in the basis set for the terminal hydride[7] in **3**, since this hydride represents the bridging hydride on **2**. The rotation of H_2 on **3** gives exactly the same shaped energy curve as for the rotation of H_2 on **2**. Again, the energy minimum occurs at $\theta = 150°$ with an energy barrier of 3.3 kcal mol^{-1}, only 0.2 kcal mol^{-1} greater than that for **2**.[10] The MOP between the closest H center of H_2 and HB is 0.017 at the total energy minimum. These facts indicate that **3** is indeed a good model for examining the rotation of H_2 on **2**. For the purposes of an accurate bonding description around the H_2 site, we can assume that the second ruthenium center in **2** acts in a passive manner; it contributes to the structure as a coercive factor, fixing the geometry of the bridging atoms. We can thus describe the bonding in **2** using **3**.

Figure 2 shows the interaction between the two fragments $[(PH_3)(NH_3)Ru(Cl)_2(H)]^-$ and H_2 at the total energy maximum ($\theta = 60°$, left-hand side) and minimum ($\theta = 150°$, right-hand side). The orbitals of the metallic fragment are derived from those of a highly distorted C_{4v} fragment. The LUMO of $[(PH_3)(NH_3)Ru(Cl)_2(H)]^-$ is an acceptor orbital, derived from the σ-hybrid of a regular C_{4v} ML_5 fragment.[11] This interacts in a stabilizing way with σ_{HH}. This interaction is essentially symmetrical with respect to the rotation of H_2, and the overlap does not change significantly as H_2 is rotated (Table I) and will not be considered any further here.

The HOMO and the second highest molecular orbital of the metal fragment are predominantly chlorine lone pairs and do not interact with any H_2 orbitals at any value of θ. They do interact in a destabilizing manner with σ_{HH} but this is independent of θ. Below these orbitals there are three metal fragment molecular orbitals that dominate the rotation of H_2 and are derived from the t_{2g} set of a regular C_{4v} ML_5 fragment. All of these orbitals are distorted with respect to an ideal octahedron and have the ability to overlap with σ^*_{HH}. The highest of these, $d_{\parallel}$, is a linear combination of *xy* and *xz*, which is destabilized by the participation of the chlorine lone pairs (**3a**). The second highest, $d_{\perp}$, is essentially *yz* and again is destabilized by chlorine lone pairs (**3b**). The third orbital is a linear combination of *xy* and *xz* and the metal hydride orbital (**3c**). We call this orbital d_{HYD}, and it is hybridized away from destabilization by the chlorine lone pairs by the participation of the metal hydride orbital.[12] This orbital is the lowest lying but is directed toward the vacant site.

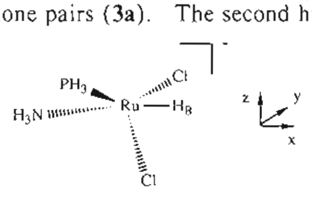

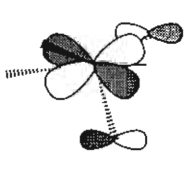

$d_{\parallel}$ **3a**

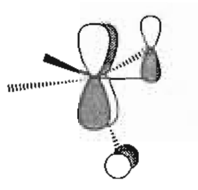

$d_{\perp}$ **3b**

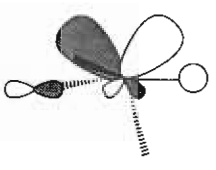

d_{HYD} **3c**

The overlap and MOP between these orbitals and σ^*_{HH} at the total energy minimum and maximum are given in Table I, and the variation in MOP is plotted in Figure 3a versus the angle of rotation θ. In Figure 3b the sum of the MOP of the three orbitals with σ^*_{HH} is plotted. This shows that the strongest overall MOP is found for $\theta = 150°$. Recall that the total energy minimum is still related to the Ru1···Ru2 direction in **2** and that $\theta = 150°$ means that the H_2 is aligned virtually in the Ru1–HB direction in **3**. At $\theta = 150°$, the total energy minimum, σ^*_{HH} overlaps with both $d_{\parallel}$ and d_{HYD}, while at $\theta = 60°$, the total energy maximum, σ^*_{HH} overlaps only with $d_{\perp}$. The overlap between d_{HYD} and σ^*_{HH} is sufficiently large to give the largest MOP even though d_{HYD} is low lying, a result of the hybridization toward the vacant site. It is this interaction that dominates the conformation of H_2.

Thus, H_2 prefers to align with a low-lying orbital that is hybridized toward σ^*_{HH} by the participation of the metal hydride

---

(9) This MOP is larger than H2···HB even though the HB···HT distance is longer because hydridic parameters have been used for HT.[7] One effect of this is to make the cis interaction more efficient.[4,5]

(10) Evans, D. G.; Mingos, D. M. P. *J. Organomet. Chem.* **1982**, *232*, 171. Evans and Mingos have suggested that hydride-like parameters are the best description of bridging hydride ligands. If such parameters are used for HB in **2** and **3**, there is no difference in the position of the energy minimum but the barriers are increased to 3.7 and 4.1 kcal mol^{-1}, respectively. Since the change in parameters causes only a marginal difference in the value of the energy barrier and no difference in the position of the energy minimum, we have used normal H parameters for all bridging hydrides, including the terminal hydride HB in **3**.

(11) Elian, M.; Hoffmann, R. *Inorg. Chem.* **1975**, *14*, 1058.

(12) The lone pair of the NH_3 group also plays a role in hybridizing d_{HYD} toward the vacant site, since this too interacts with the metal hydride orbital. This is similar to the effect of a distorted phosphine.[4]

Table II. Overlaps and MOPs between Fragment Molecular Orbitals of $(PH_3)_2(H)Ru(\mu\text{-}H)_3Ru(PH_3)_2$ and H_2 in **3** at $\theta = 0°$ (Total Energy Maximum) and at $\theta = 90°$ (Total Energy Minimum)

	$\theta = 0°$	$\theta = 90°$
	Overlap	
$\langle \sigma_{HH} \mid LUMO \rangle$	0.235	0.234
$\langle \sigma^*_{HH} \mid$ **5a** $\rangle$	0.159	0.000
$\langle \sigma^*_{HH} \mid$ **5b** $\rangle$	0.000	0.186
$\langle \sigma^*_{HH} \mid$ **5c** $\rangle$	0.127	0.000
	MOP	
$\langle \sigma^*_{HH} \mid$ **5a** $\rangle$	0.055	0.000
$\langle \sigma^*_{HH} \mid$ **5b** $\rangle$	0.000	0.074
$\langle \sigma^*_{HH} \mid$ **5c** $\rangle$	0.034	0.000

bond. This is clearly a prime example of the cis effect of a hydride ligand on the orientation of H_2.

Another interesting feature of **1** is that, although the complex is fluxional, only one of two potential isomers is observed. We have examined this second isomer using **2′**, $(PH_3)(NH_3)(H)Ru(\mu\text{-}Cl)_2(\mu\text{-}H)Ru(PH_3)_2(\eta^2\text{-}H_2)$, which would be found at the other end of the exchange process of **2**. Effectively in **2′** H_2 and HT have exchanged sites; we find an energy difference between **2** and **2′** of 9.4 kcal mol^{-1} in favor of **2**.

A close examination of these two sites can provide a simple explanation for this absence of evidence for **2′**. If in both **2** and **2′** we assume that H_2 aligns with the Ru–HB bond, then the ligand trans to the bridging hydride may provide the contrast between the two isomers. In the case of Ru1, the ligand trans to HB is an NH_3 group, bent *away* from H_2 (98.6°) helping to hybridize d_{HYD} *toward* σ^*_{HH}. Conversely, the ligand trans to HB on Ru2 is a PH_3 group, which is bent up *toward* the H_2 (81.3°) and thus hybridizing d_{HYD} *away* from σ^*_{HH}. Therefore, by exchanging H_2 and HT on the two metal centers, we move H_2 from a site where the trans ligand optimizes H_2 coordination (Ru1) to a site where it is unfavorable (Ru2). These comments are purely speculative, since they do not allow for any relaxation of the geometry of the complex during the exchange, but they do account for the observation of one single isomer.

H_2 Coordination on $(PR_3)_2(H)Ru(\mu\text{-}H)_3Ru(PR_3)_2(H_2)$

The other dinuclear complex that has been proposed to include nonclassically coordinated H_2 is $(PR_3)_2(H)Ru(\mu\text{-}H)_3Ru(PR_3)_2(H_2)$ (**4**) (R = Cy).[2a] Although NMR measurements indicate the presence of nonclassical H_2, no crystal structure has been performed to data and the exact structure remains unknown. The NMR measurements also indicate that all the hydrides are highly fluxional.

We have examined the rotation of H_2 on $(PH_3)_2(H)Ru(\mu\text{-}H)_3Ru(PH_3)_2(H_2)$ (**5**) with a totally symmetric C_s structure,[6] placing the terminal hydride on the same side of the dimer as both the nonclassical H_2 and two of the bridging hydrides. Hydridic parameters were used for the terminal hydride, and normal hydrogen parameters, elsewhere in the complex.[7] Although such a structure has not been proved, it seems highly likely in view of the facile exchange processes occurring. We have used a Ru–HB–Ru angle of 120°[13] and a HB···HB distance of 1.42 Å. The structure has a Ru···Ru nonbonding distance of 2.84 Å.[14]

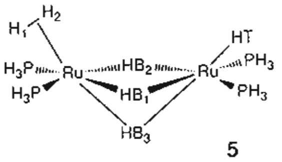

5

The barrier to rotation of H_2 on **5** is 0.9 kcal mol^{-1}, and at the total energy minimum the H_2 bond aligns with the Ru···Ru direction, i.e. bisecting the two Ru–HB vectors ($\theta = 90°$). The MOP between the closest atom of H_2 and HB1 (HB2) at the total energy minimum is 0.010, which is a magnitude indicative of the presence of a cis interaction. However, we also notice that at the total energy maximum ($\theta = 0°$) there is a MOP of 0.007 between H1 (H2) and HB1 (HB2). In this case the molecular H_2 is parallel to the HB1···HB2 direction. We will start by examining the bonding using a fragment molecular orbital analysis between metal fragment, $(PH_3)_2(H)Ru(\mu\text{-}H)_3Ru(PH_3)_2$, and H_2. As in **3**, the LUMO of the metal fragment interacts with σ_{HH}, an interaction that is symmetrical with respect to the rotation of H_2 (see the overlaps in Table II) and does not contribute to the conformational preferences.

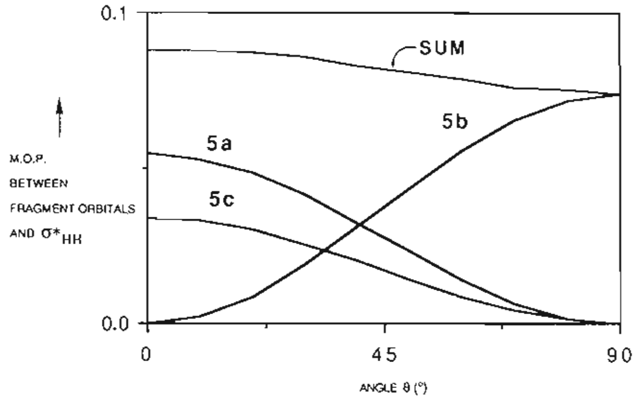

Figure 4. Variation in MOP of the d orbitals of **5** with σ^*_{HH}, separately and summed (top trace), with changing θ.

There are three fragment molecular orbitals that have the potential to overlap with σ^*_{HH}. Associated overlaps and MOP are given in Table II. The highest of these orbitals, **5a**, is a combination of $x^2 - y^2$, xy, and metal hydride orbitals and is thus an $x^2 - y^2$ type orbital including Ru–HB bonds to the two bridging hydrides nearest to H_2. This orbital overlaps with σ^*_{HH} when $\theta = 0°$ (Table II). The second highest orbital, **5b**, is a mixture of yz and metal hydride orbitals, hybridized toward H_2, having a maximum overlap with σ^*_{HH} at $\theta = 90°$ and a minimum at $\theta = 0°$. The third fragment molecular orbital, **5c**, is also a combination of $x^2 - y^2$, xz, and metal hydride orbitals and is thus a z^2 type orbital associated with bonding to the single bridging hydride on the opposite side of the dimer to H_2. When $\theta = 0°$, **5c** overlaps to a lesser extent with σ^*_{HH} than **5a**.

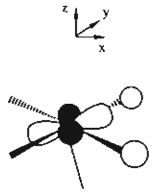

5a

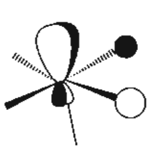

5b

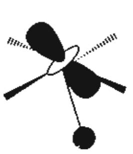

5c

Figure 4 shows the variation of the MOP of the three orbitals **5a**, **5b**, and **5c** with θ, along with the sum of the MOP of the three orbitals, which shows that while **5b** has the largest single MOP, at $\theta = 90°$, the sum of the other two MOPs at $\theta = 0°$ is larger than this and these two orbitals dominate the rotation. All of these orbitals have high coefficients on the bridging hydrides, which contribute toward the MOP between the dihydrogen and the bridging hydrides at all angles of rotation.

It is again a cis interaction that dominates the rotation of H_2 on this dinuclear complex. However, the barrier is very small, and this appears to be due to two factors. First, unlike **2** and **3**, no distortion of the octahedral environment has been introduced into the calculation for **5**. We have previously shown that it is necessary to take into account the precise position of phosphine ligands to explain the orientation of H_2.[4b] Second, because there are *two* hydrides cis to H_2, they start to have the reverse effect, since metal–hydride bonds have the symmetry to interact with more than one metal orbital. This means that the presence of

---

(13) We have chosen 120°, since it is close to the Ru1–HB–Ru2 angle in **1**,[3] which is 122°, and gives reasonable MOPs for both the Ru···Ru interaction and the HB···HB interaction.

(14) The MOP between the two rutheniums in **5** is 0.060 compared to that in **2**, where the same MOP is 0.017.

the second hydride reduces the barrier to rotation by the very same effect that increased it in the first place.

There is another interesting feature of this complex, namely the interactions between the three bridging hydrides. A thorough theoretical analysis of dinuclear complexes with bridging hydrides has been previously carried out.[15] The possibility of three bridging hydrides having real chemical bonds between them, and hence being a "trihydrogen" fragment, has also been discussed.[16] Such an interaction was concluded to be highly improbable by later workers.[17] The three bridging hydrides in **5** form an equilateral triangle in our calculation with side length of 1.42 Å. We find a MOP between these hydrides at 0.047 between HB3 and HB1 (HB2) and 0.039 between HB1 and HB2. These MOP values indicate that there is some sort of positive interaction between these bridging hydrides but by no means on the scale of a trihydrogen complex.

Conclusions

We conclude that the conformation of nonclassical H_2 on a metal center in dinuclear transition-metal complexes is influenced by the same factors as in mononuclear complexes. Here these factors are the attractive effect of a hydride cis to the site of H_2 and the optimization of metal–σ^*_{HH} back-bonding. Bridging hydrides are found to be equally as capable of having an attractive cis effect as terminal hydrides. The distortion of the ligand field can also hybridize the metal d orbitals to give optimum conditions for metal to H_2 back-bonding. It is important to take into account the exact positions of all the ligands around the metal, since some of the d orbitals are thus distorted to become stronger or weaker candidates for back-bonding into σ^*_{HH}. Apparently the orientation of H_2 is very sensitive to all these factors. The low barriers to rotation of the ligand H_2 in its complexes are derived from the high energy of σ^*_{HH}, leading to a weak interaction with the occupied metal orbitals.

The cis interaction induces a nascent bond between an H of H_2 and the closest (terminal or bridged) hydride. We have already suggested that this nascent bond is likely to be a factor that might lower the activation energy of intramolecular H exchange. In mononuclear complexes this exchange could be viewed as site exchange between molecular H_2 and terminal H, accompanied by H center scrambling. If a similar process is operating in dinuclear complexes, then it is possible that molecular H_2 could bridge two metals. We certainly have no evidence for such a species, but the fact that diatomics such as CO or N_2 are known to bridge two metals gives some support to this hypothesis. Related structures have just been proposed to explain the exchange process in $Re_2H_8(PPh_3)_4$.[18]

Acknowledgment. We wish to thank the CNRS and the EEC for a postdoctoral fellowship (S.A.J.). The Laboratoire de Chimie Thêorique is associated with the CNRS, URA 506, and is a member of ICMO and IPCM.

---

(15) Dedieu, A.; Albright, T. A.; Hoffmann, R. *J. Am. Chem. Soc.* **1979**, *101*, 3141.

(16) Burdett, J. K.; Pourian, M. R. *Organometallics* **1987**, *6*, 1684.

(17) Bianchini, C.; Laschi, F.; Masi, D.; Mealli, C.; Meli, A.; Ottaviani, F. M.; Proserpio, D. M.; Sabat, M.; Zanello, P. *Inorg. Chem.* **1989**, *28*, 2552.

(18) Cotton, F. A.; Luck, R. L. *Inorg. Chem.* **1989**, *28*, 4527.

Additions and Corrections

1990, Volume 29

D. Min, R. D. Larsen, K. Emerson, and E. H. Abbott*: Synthesis and Crystal and Molecular Structures of Potassium Bis(μ-hydroxo)bis[dinitritoplatinate(II)] Sesquihydrate and Potassium *cyclo*-Tris(μ_3-oxo-1:2:4;1:3:4;2:3:4)tris[dinitritoplatinate(II)]trinitritoplatinate(IV) Trihydrate.

Pages 73–76. We wish to call the attention of the readers to the fact that potassium *cyclo*-tris(μ_3-oxo-1:2:4;1:3:4;2:3:4)tris[dinitritoplatinate(II)]trinitritoplatinate(IV) trihydrate, one of the compounds whose crystal and molecular structure we discussed, was first reported by Koz'min and co-workers (Koz'min, P. A.; Lapkin, V. V.; Shubochkin, L. K.; Surazhakaya, M. D.; Subochkina, E. F.; Larina, T. B. *Russ. J. Inorg. Chem.* (*Engl. Transl.*) **1988**, *33*, 532; *Dokl. Chem.* (*Engl. Transl.*) **1986**, *286*, 125). Also, Professor Koz'min has reported infrared and partial structural data on bis(μ-hydroxo)bis[dinitritoplatinate(II)] (Koz'min, P. A.; Lapkin, V. V.; Surazhakaya, M. D.; Shubochkin, L. K.; Larina, T. B.; Shubochkina, E. F. *Russ. J. Inorg. Chem.* (*Engl. Transl.*) **1986**, *31*, 1177). Our work confirms structural suggestions contained in his paper.—E. H. Abbott